CHAPTER TWO

BIOMIMETIC PARTIAL SYNTHESIS OF VALPARICINE AND APPARICINE

2.1 Introduction

2.1.1 Alkaloids of *Kopsia arborea*

A total of 62 alkaloids were isolated from the stem-bark and leaves of *Kopsia arborea* of which 25 are new alkaloids. Among the alkaloids isolated are valparicine (**28**),[26,27] pericine (**31**),[26,28,29] pericidine (**32**),[30,31] arbophylline (**33**),[32] arboricine (**34**),[30,33] arboricinine (**35**),[30,33] arboflorine (**36**),[30,34] arboloscine (**37**),[30,31] and mersicarpine (**38**).[35]

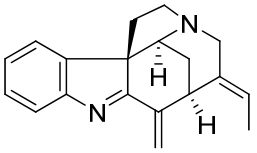

28 Valparicine

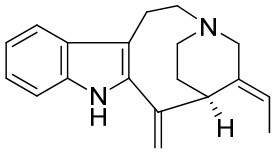

31 Pericine

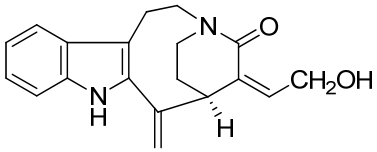

32 Pericidine

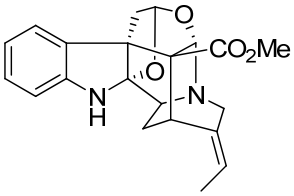

33 Arbophylline

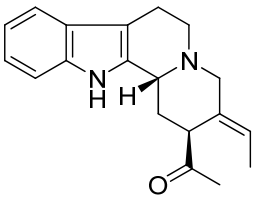

34 Arboricine

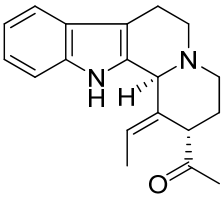

35 Arboricinine

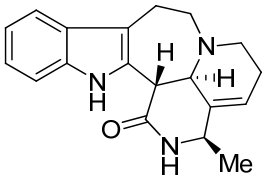

36 Arboflorine

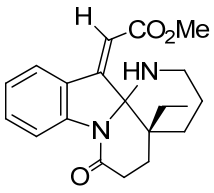

37 Arboloscine

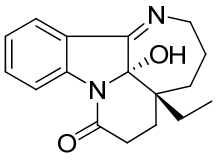

38 Mersicarpine

The compounds of interest to this research are valparicine (**28**) and pericine (**31**).

Valparicine (**28**) was isolated from the stem-bark extract of *K. arborea* in trace amount. It represents the first member of the pericine-type alkaloids, characterized by a 16-22 exocyclic double bond, in which bond-formation has occurred between C-3 and C-7.[26] Preliminary tests indicated that valparicine (**28**) showed strong cytotoxic effects against human KB cells ($IC_{50} < 5\ \mu gmL^{-1}$).

Valparicine (**28**) was obtained as a colorless oil, with $[\alpha]_D$ –40 (*c* 0.22, $CHCl_3$). The UV spectrum (228 and 297 nm) indicated the presence of an unsubstituted indolenine chromophore. The EIMS of **28** showed a molecular ion at *m/z* 276, which analyzed for $C_{19}H_{20}N_2$, differing from pericine (**31**) by loss of two hydrogens. The ^{13}C NMR spectrum gave a total of 19 carbon resonances (one methyl, five methylenes, seven methines, and six quaternary carbons) in agreement with the molecular formula. In addition to the six carbon resonances readily attributable to the aromatic moiety, and the imine resonance at δ_C 186.4, two other downfield quaternary resonances were observed at δ_C 139.2 and 144.6. The former was associated with an ethylidene side chain, as shown by the characteristic H signals at δ_H 5.52 (qd) and 1.78 (d). The other was associated with an exocyclic double bond, from the two broad singlets observed at δ_H 5.39 and 6.02, due to the geminal hydrogens of C-22 (δ_C 116.4). The remaining quaternary carbon resonance at δ_C 65.1 was attributed to the indole C-7. The NMR spectroscopic data of **28** revealed a similarity with the stemmadenine-type alkaloid, **31**. The major departure noted from the NMR data of **28** was the formation of a bond between C-3 to the indole C-7, and the change from an indole to an indolenine chromophore. The ^1H and ^{13}C NMR spectral data of **28** are summarized in Table 2.1, and the ^1H and ^{13}C NMR spectra for **28** are shown in Fig. 2.1 and Fig. 2.2, respectively.

The other alkaloid of interest, pericine (**31**), was isolated as one of the major alkaloids from *K. arborea*.[26] Pericine (**31**) was first isolated in 1982 from *Picralima*

nitida cell suspension cultures[28] and subsequently (2002) from *Aspidosperma subincanum* under the name, subincanadine.[29]

Pericine (**31**) was obtained as a light yellowish oil, with $[\alpha]_D$ +45 (*c* 0.20, $CHCl_3$). The UV spectrum (226 and 301 nm) suggested the presence of an indole chromophore. The ESIMS of **31** showed an MH^+ at *m/z* 279, consistent with the molecular formula $C_{19}H_{23}N_2$. In agreement with this, the ^{13}C NMR spectrum showed a total of 19 carbon resonances (one methyl, six methylenes, six methines, and six quaternary carbons). The ^1H NMR spectrum of **31** showed, in addition to the resonance due to NH (δ_H 8.02) and four aromatic hydrogens of an unsubstituted indole chromophore (δ_H 7.49, H-9; δ_H 7.10, H-10; δ_H 7.18, H-11; δ_H 7.31, H-12), a characteristic pair of one-H doublets at δ_H 5.35 and δ_H 5.36 (J = 1.5 Hz), due to the geminal hydrogens of an exocyclic double bond. The ^1H and ^{13}C NMR spectral data of **31** are summarized in Table 2.1 and the ^1H and ^{13}C NMR spectra of **31** are shown in Fig. 2.3 and Fig. 2.4, respectively.

The promising bioactivity of valparicine (**28**) requires that sufficient amounts should be available for further evaluation of its cytotoxic effects. Since compound **28** was isolated only in trace amount from its natural source, a viable semi-synthetic route to **28** is required. It occurred to us that a possible route to valparicine (**28**) is from the stemmadenine-type alkaloid, pericine (**31**), via generation of the C(3)-N(4) iminium ion, followed by intramolecular ring closure (vide infra). It also occurred to us that pericine (**31**) may also be of relevance to the biosynthesis of the 5-*nor*-indole alkaloid, apparicine (**29**). In the following section we shall consider the biogenetic relationship between stemmadenine (**13**), vallesamine (**39**), apparicine (**29**), and pericine (**31**).

Table 2.1: ^{1}H and ^{13}C NMR Spectroscopic Data of Valparicine (**28**) and Pericine (**31**)[a]

Position	**28**		**31**	
	^{1}H	^{13}C	^{1}H	^{13}C
2	-	186.4	-	135.2
3	4.10 s	65.1	2.81 m	45.3
	-		3.13 m	
5	3.23 ddd (11, 6.5, 4.1)	56.5	3.12 m	57.8
	3.36 ddd (11, 9.2, 6.1)		3.26 m	
6	1.97 ddd (12.9, 6.1, 4.1)	36.7	2.78 m	24.3
	2.42 ddd (12.9, 9.2, 6.5)		3.50 ddd (15, 11, 3)	
7	-	65.1	-	112.4
8	-	144.5	-	128.5
9	7.37 d (7.5)	121.0	7.49 d (8)	118.5
10	7.22 td (7.5, 1)	125.8	7.10 ddd (8, 7, 1)	119.3
11	7.34 td (7.5, 1)	127.9	7.18 ddd (8, 7, 1)	122.2
12	7.61 d (7.5)	120.7	7.31 m	110.4
13	-	154.2	-	135.3
14	2.01 dt (14.2, 3.2)	27.0	1.66 m	27.7
	1.38 dt (14.2, 2.7)		2.10 dddd (15, 11, 8, 7)	
15	3.85 s	37.3	3.98 br d (6.4)	42.8
16	-	144.6	-	145.4
18	1.78 d (7)	13.7	1.69 dt (7, 1)	13.4
19	5.52 qd (7, 1.3)	119.8	5.62 q (7)	120.8
20	-	139.2	-	138.8
21	3.77 dt (15.0, 1.6)	54.5	3.26 m	53.8
	3.29 d (15.0)		3.88 d (16.3)	
22	5.39 s	116.4	5.35 d (1.5)	117.6
	6.02 s		5.36 d (1.5)	
NH	-	-	8.02 br s	-

[a] $CDCl_3$, 400 MHz

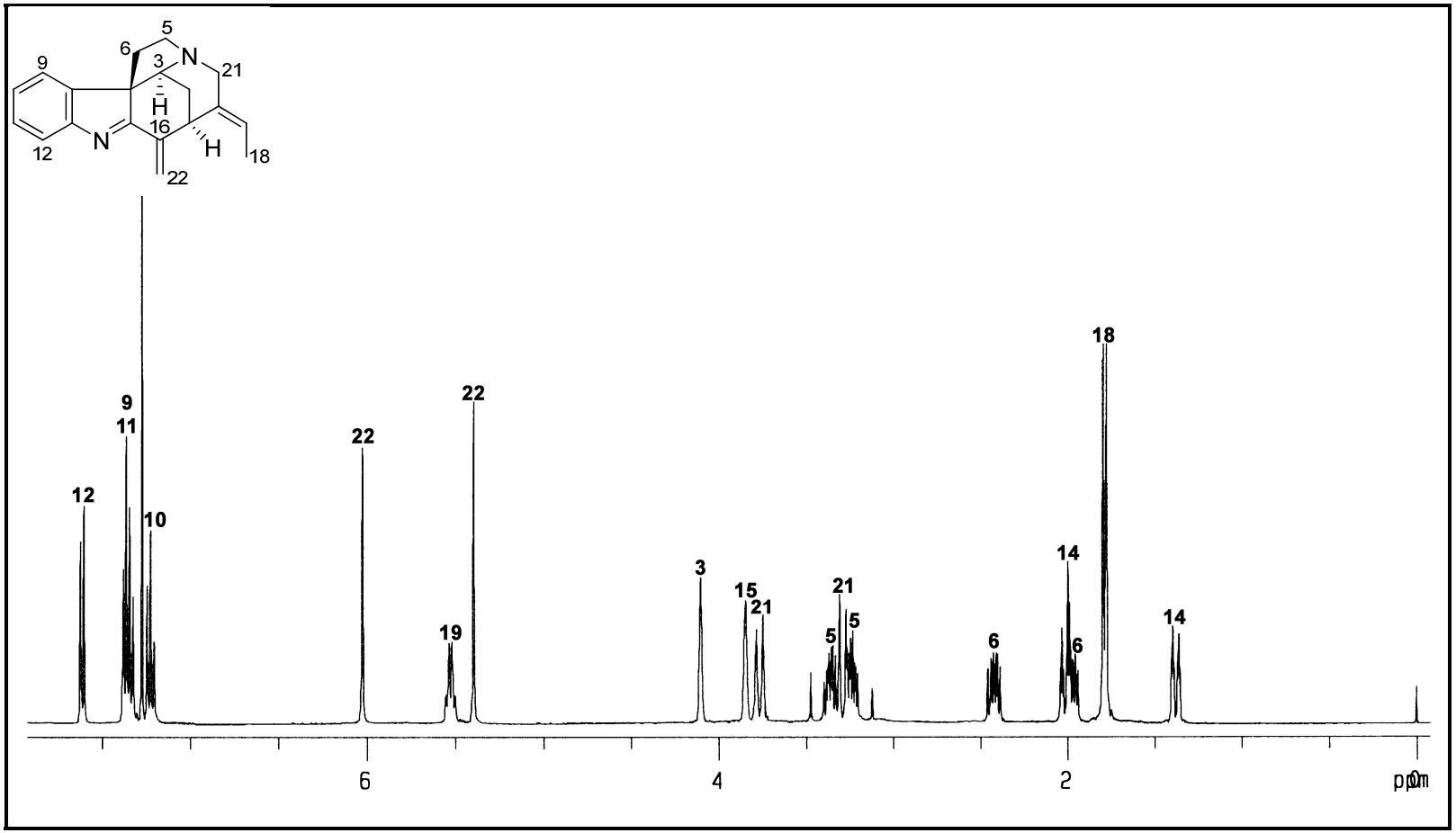

Fig. 2.1: ^{1}H NMR Spectrum ($CDCl_3$, 400 MHz) of Valparicine (**28**)

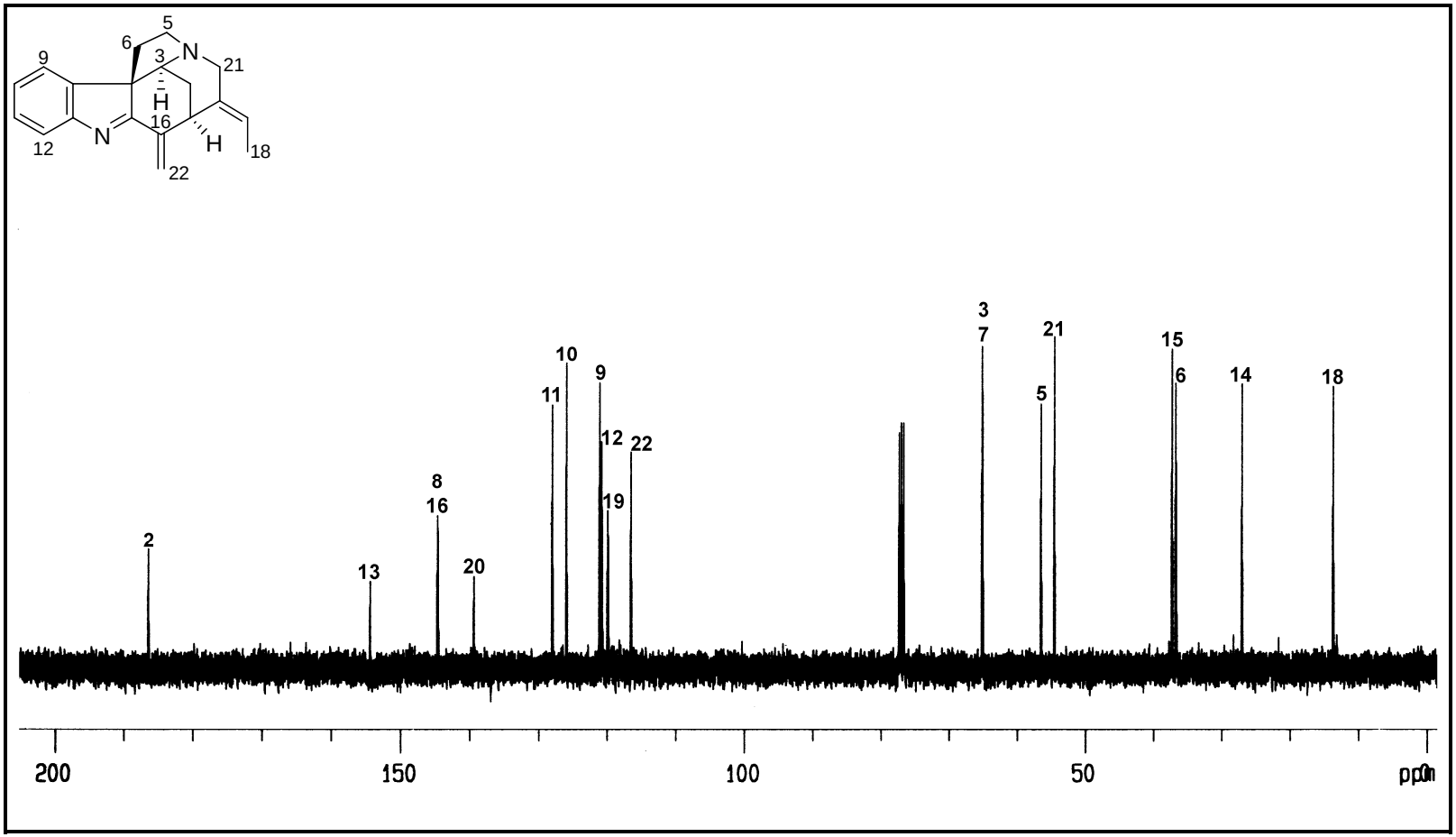

Fig. 2.2: ^{13}C NMR Spectrum ($CDCl_3$, 100 MHz) of Valparicine (**28**)

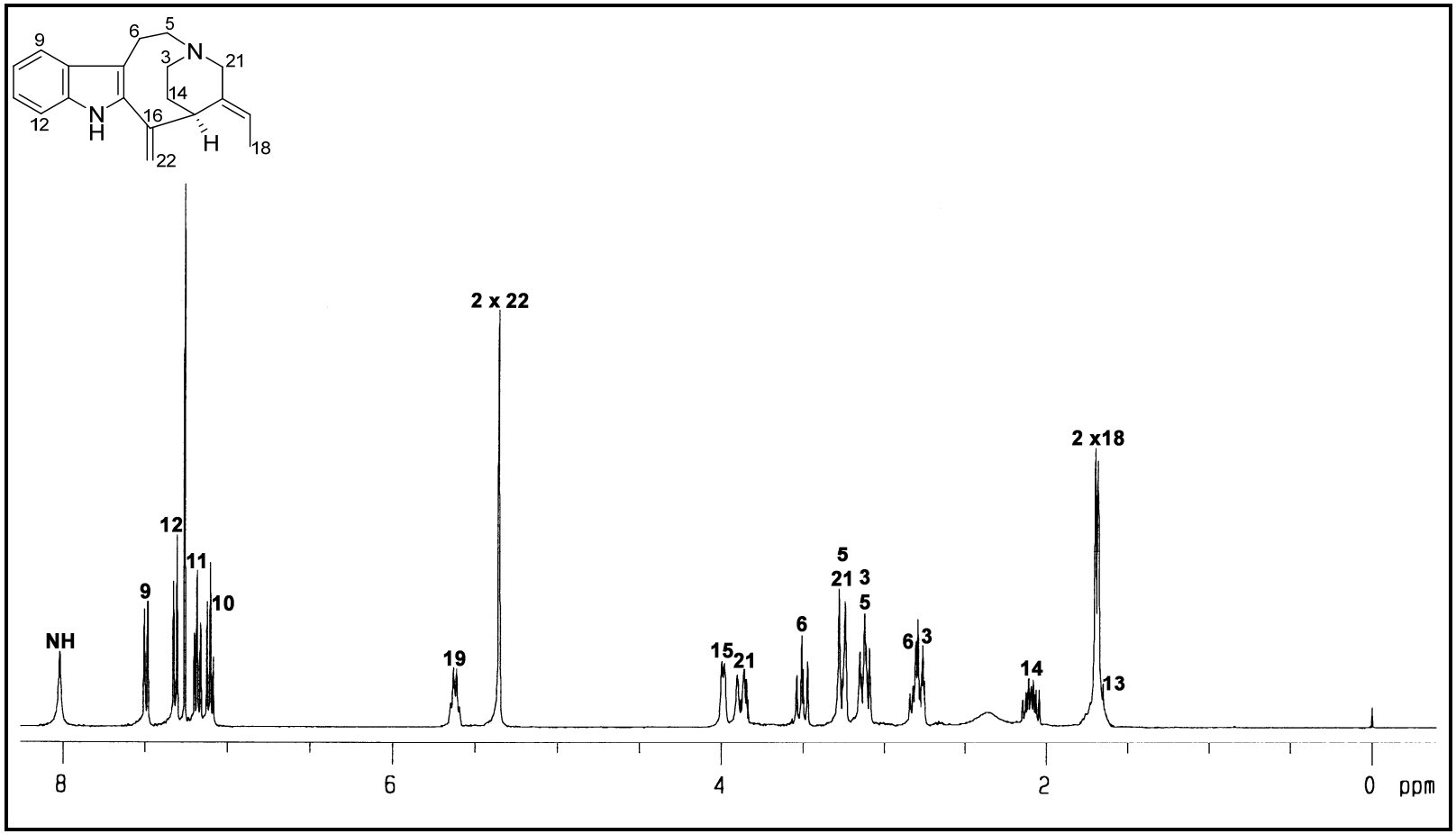

Fig. 2.3: ^{1}H NMR Spectrum ($CDCl_3$, 400 MHz) of Pericine (**31**)

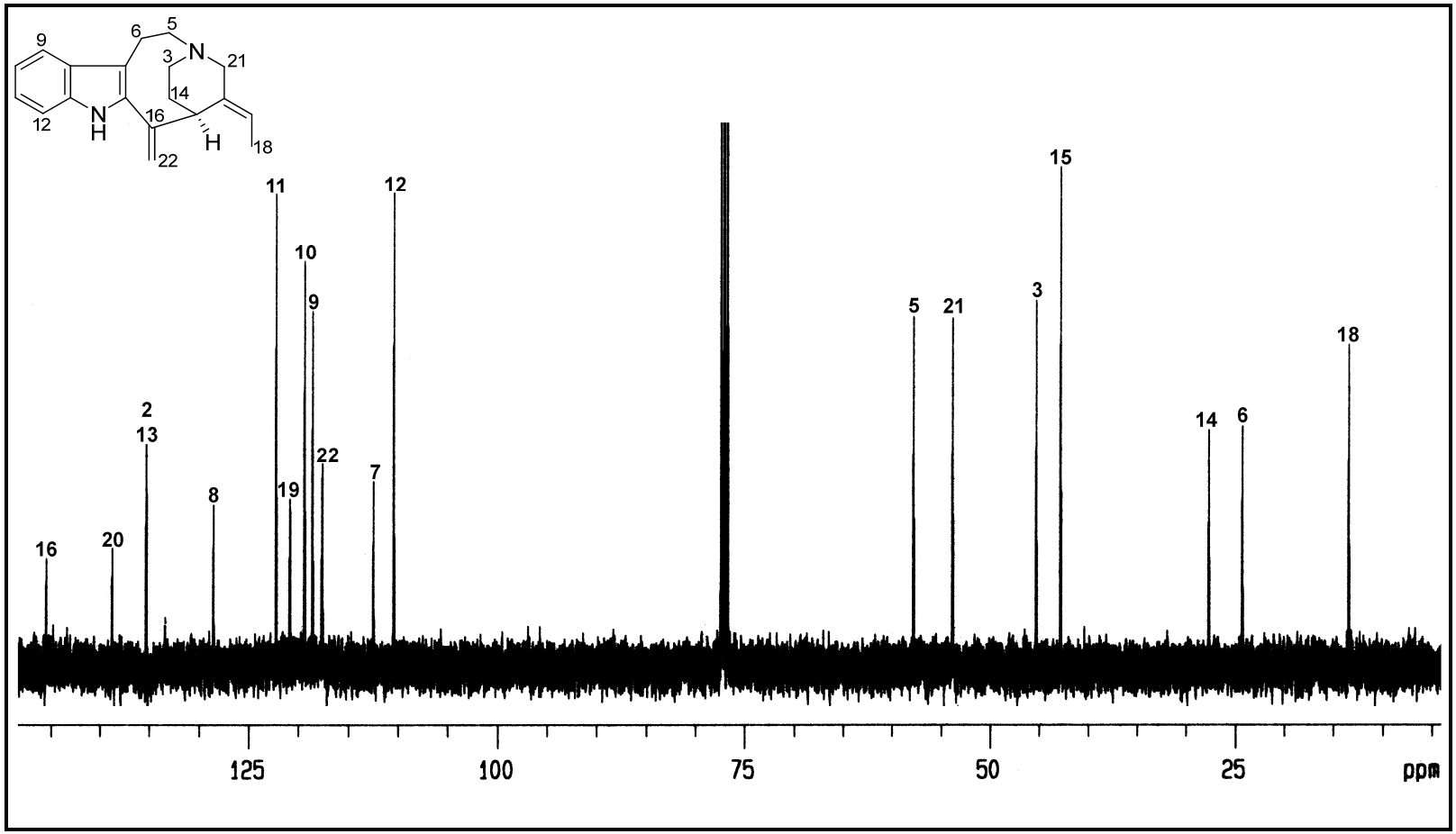

Fig. 2.4: ^{13}C NMR Spectrum ($CDCl_3$, 100 MHz) of Pericine (**31**)

2.1.2 Biogenesis of Apparicine (29)

Apparicine (**29**), the first indole alkaloid having only one of the two tryptamine-derived side chain carbons, was first isolated from *Aspidosperma dasycarpon*.[36] Apparicine (**29**) is notable for its pronounced analeptic properties, being a convulsant of the tonic/colonic variety in mice at doses as low as 2 $mgkg^{-1}$.[37]

Apparicine (**29**) was isolated as a light yellowish oil, $[\alpha]_D$ −177 (*c* 0.03, $CHCl_3$). The mass-spectrum (ESIMS) of **29** displayed an MH^+ at *m/z* 265, consistent with the molecular formula $C_{18}H_{21}N_2$. The ^1H NMR spectrum showed the presence of four aromatic protons from δ_H 7.06 to 7.41, an indolic NH at δ_H 7.92, and an ethylidene side chain (δ_H 1.46 and 5.27). A conspicuous feature of the ^1H NMR spectrum is the presence of two exocyclic methylene proton singlets (H-22) at δ_H 5.26 and 5.40. The ^{13}C NMR spectrum showed a total of 18 carbon resonances, which were classified into one methyl, five methylenes, six methines, and six quaternary carbons. The ^1H and ^{13}C NMR spectral data for **29** are summarized in Table 2.2, and the ^1H and ^{13}C NMR spectra of **29** are shown in Fig. 2.5 and Fig. 2.6, respectively.

Table 2.2: ^{1}H and ^{13}C NMR Spectroscopic Data of Apparicine (**29**)[a]

Position	^{1}H	^{13}C
2	-	137.6
3	3.07 dddd (13, 9, 7, 2)	45.3
	3.43 ddd (13, 8, 2.5)	
6	4.26 d (17.6)	54.1
	4.52 d (17.6)	
7	-	110.9
8	-	129.0
9	7.41 br d (8)	118.6
10	7.06 ddd (8, 7, 1)	119.3
11	7.18 ddd (8, 7, 1)	123.0
12	7.29 dt (8, 1)	110.2
13	-	135.6
14	1.90 ddt (13, 7, 2.5)	29.5
	2.17 dddd (13, 9, 8, 5)	
15	3.92 br s	41.2
16	-	145.1
18	1.46 dd (6.8, 2)	12.5
19	5.27 q (6.8)	120.3
20	-	131.9
21	3.21 br d (15)	54.3
	3.82 dt (15, 2)	
22	5.26 s	112.3
	5.40 s	
NH	7.92 br s	-

[a] $CDCl_3$, 400 MHz

The biogenetic relationship between stemmadenine (**13**) and the 5-*nor*-indole derivatives, vallesamine (**39**) and apparicine (**29**) was first suggested by Kutney, who showed that the one-carbon bridge in **29** was C-6, following excision of C-5 from the original two-carbon tryptamine bridge.[38,39] An attractive pathway from stemmadenine (**13**) to apparicine (**29**) was first put forward by Potier and coworkers (Scheme 2.1, A),

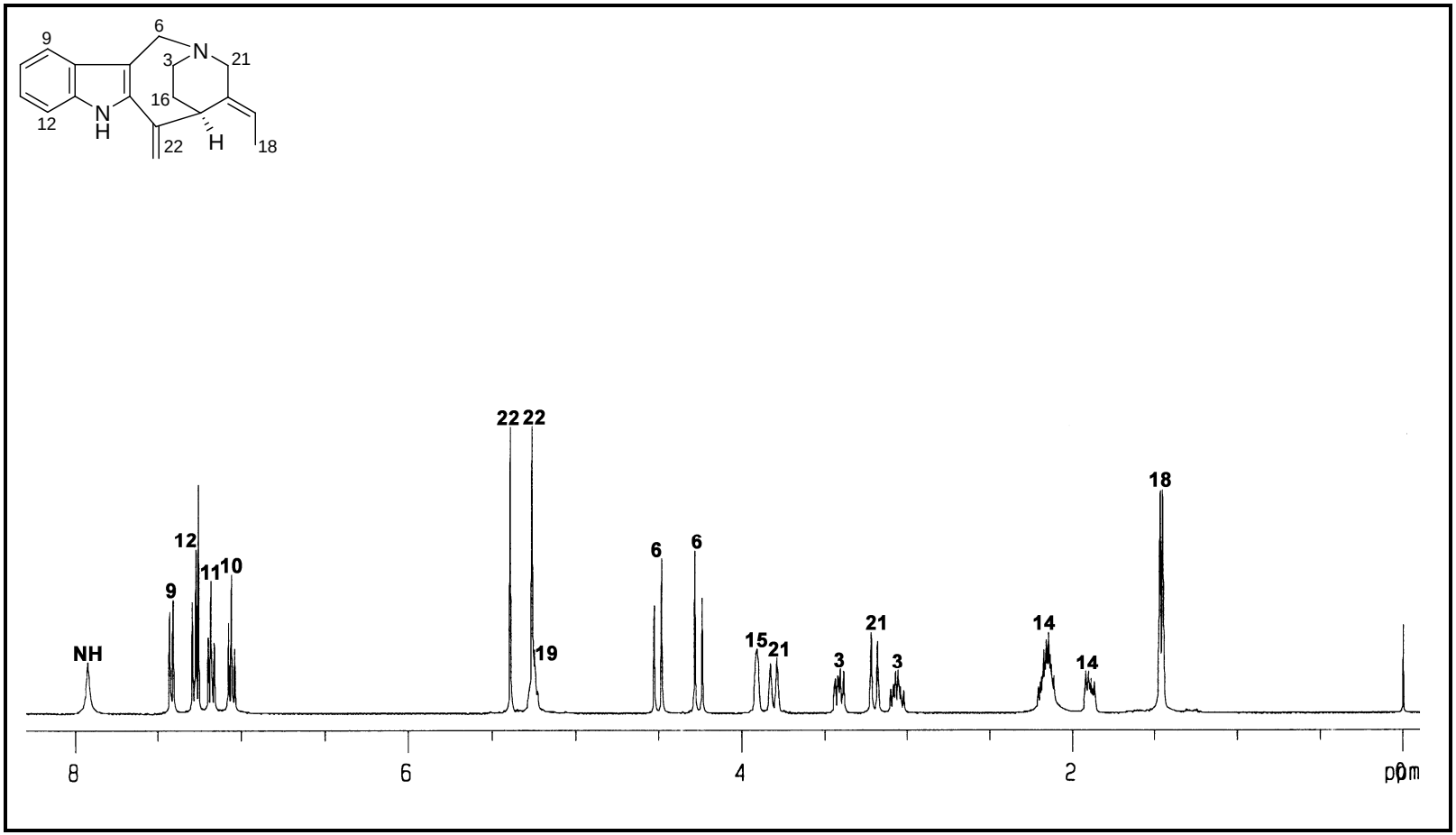

Fig. 2.5: ^{1}H NMR Spectrum ($CDCl_3$, 400 MHz) of Apparicine (**29**)

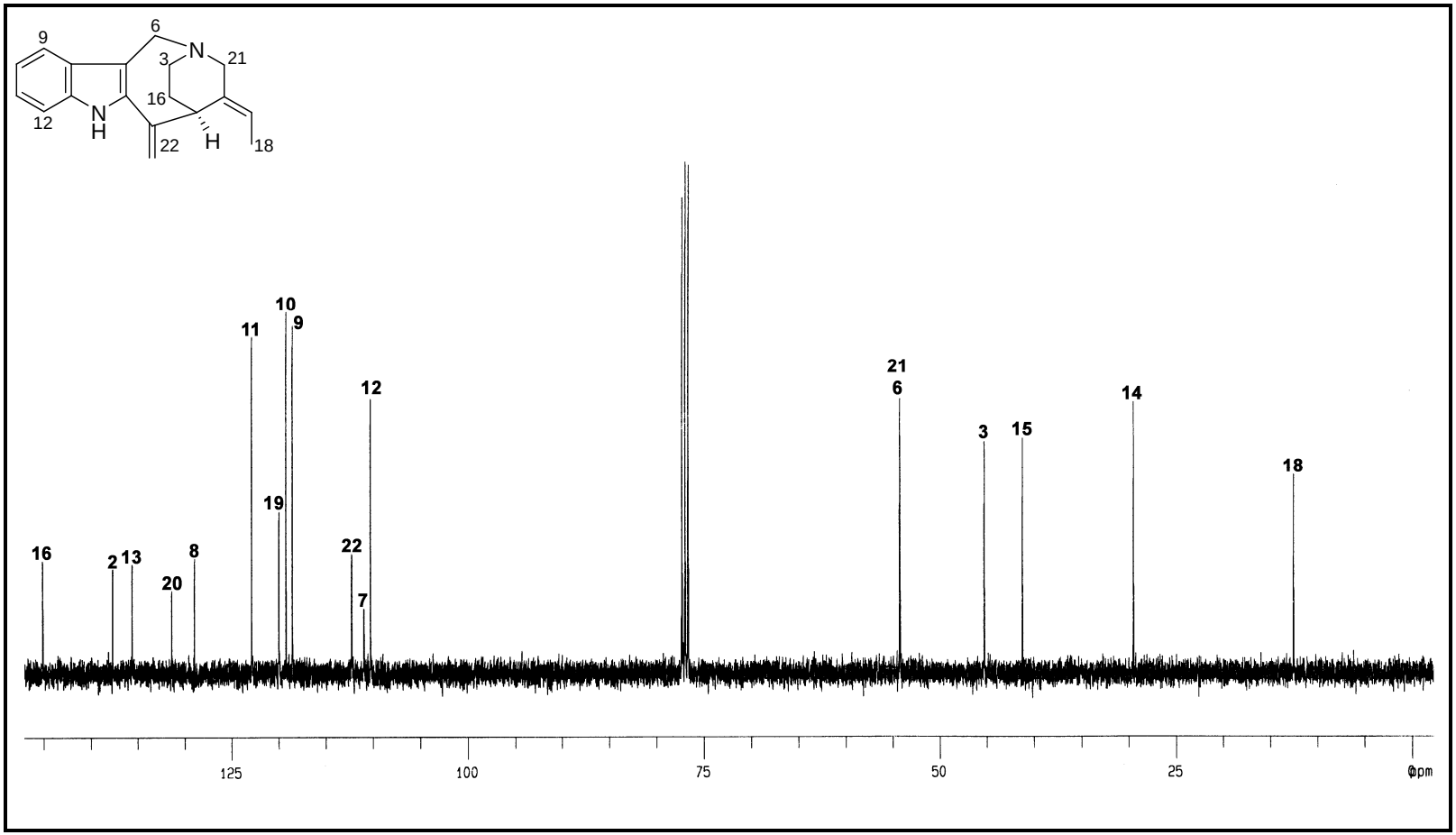

Fig. 2.6: ^{13}C NMR Spectrum ($CDCl_3$, 100 MHz) of Apparicine (**29**)

based on a route featuring the Potier-Polonovski fragmentation of the indole alkaloid N-oxide precursor.[40] A subsequent demonstration of the stemmadenine (**13**) to apparicine (**29**) transformation by Scott and coworkers (Scheme 2.1, B) provided strong support for the Potier proposal, requiring, however a modification that the decarboxylation or deformylation step need not be synchronous with fragmentation to the iminium ion.[41]

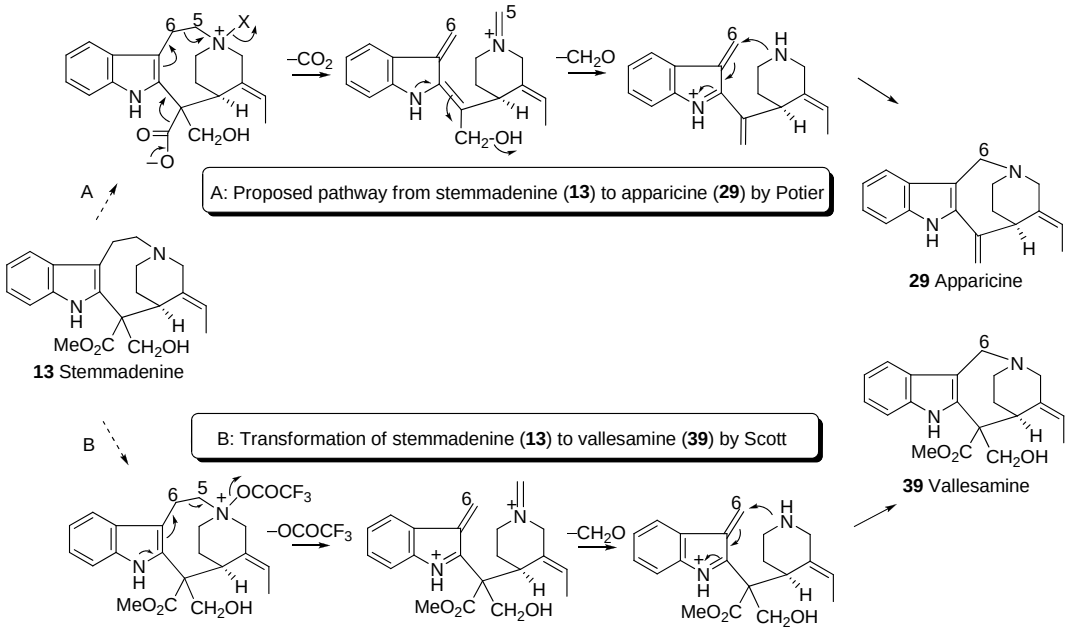

Scheme 2.1

2.1.3 Proposed Transformation of Pericine (31) to Valparicine (28) and Apparicine (29)

Based on the proposed stemmadenine (**13**) to apparicine (**29**) transformation put forward by Potier, it occurred to us that the stemmadeinine-like alkaloid, pericine (**31**) might be a possible precursor to apparicine (**29**), based on the Potier model for C-ring contraction (via the dication **40**). It also occurred to us, based on certain observations (vide infra), that valparicine (**28**) could also be formed via generation of the C(3)-N(4)

iminium ion (**41**) from the pericine *N*-oxide precursor, followed by intramolecular ring closure (Scheme 2.2).

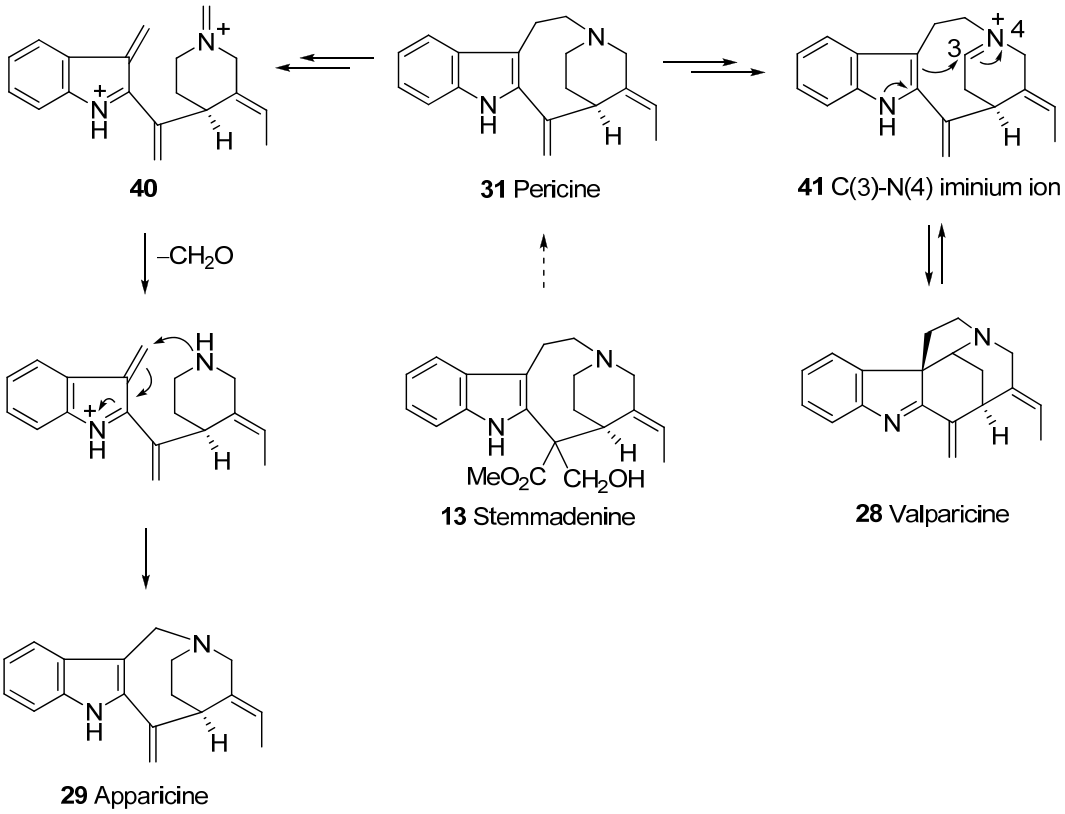

Scheme 2.2

With sufficient amounts of the requisite precursor to hand from our ongoing work in alkaloid chemistry, it remains to obtain experimental support for the proposal.

2.2 Results and Discussion

2.2.1 Preliminary Observations on the Behavior of Valparicine (28) under Various Conditions

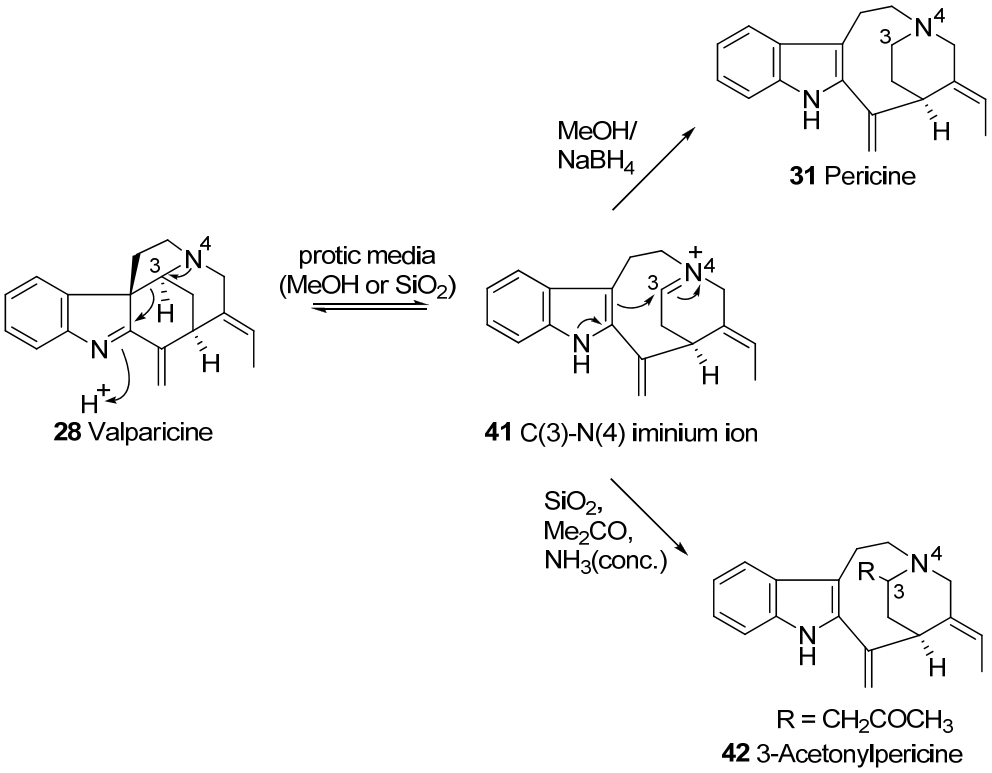

Scheme 2.3

It was frequently observed during the isolation and purification of valparicine (**28**) that the TLC chromatograms of pure **28** invariably displayed two spots, although only one compound was always recovered. This observation suggested that **28** is in equilibrium with its iminium ion **41** in protic media (Scheme 2.3).

The iminium ion **41** can also be trapped by sodium borohydride ($NaBH_4$).[42] Thus when **28** was dissolved in MeOH and $NaBH_4$ was added, pericine (**31**) was the sole product isolated (Scheme 2.3).

The iminium ion **41** can also be trapped as the 3-acetonyl derivative **42** on exposure of **28** to silica gel and acetone in the presence of a trace amount of concentrated ammonia (Scheme 2.3).

3-Acetonylpericine (**42**) was obtained as colorless prisms from acetone (mp 193−194 °C), with $[\alpha]_D$ +51 (*c* 0.20, $CHCl_3$). The IR spectrum showed, in addition to the usual indolic NH (3339 cm^{-1}), the presence of a carbonyl band (1700 cm^{-1}) which is due to the acetonyl carbonyl. The EIMS of **42** showed an M^+ at *m/z* 334, which analyzed for $C_{22}H_{26}N_2O$, i.e., 56 mass units higher than that of **31** ($M - CH_2COCH_3$). The ^{13}C NMR spectrum showed a total of 22 carbon resonances (two methyl, six methylenes, seven methines, and seven quaternary carbons), with the characteristic carbonyl resonance seen at δ_C 208.6. A conspicuous departure in the ^1H NMR spectrum of **42** when compared with that of **31** is the presence of the characteristic methyl singlet of the acetonyl group at δ_H 1.93. Compound **42** was therefore readily identified as the acetonyl derivative of **31**. The ^1H and ^{13}C NMR spectral data of **42** are summarized in Table 2.3, and the ^1H and ^{13}C NMR spectra of **42** are shown in Fig. 2.7 and Fig. 2.8, respectively.

Table 2.3: ^{1}H and ^{13}C NMR Spectroscopic Data of 3-Acetonylpericine (**42**)[a]

Position	^{1}H	^{13}C
2	-	134.9
3	3.36 dq (12.5, 6.2)	51.5
5	3.14 m	57.6
	3.21 m	
6	2.68 ddd (14.7, 3.7, 2.0)	24.1
	3.49 ddd (14.7, 12.1, 3.1)	
7	-	112.5
8	-	128.5
9	7.47 d (7.9)	118.4
10	7.08 ddd (7.9, 7.1, 1.1)	119.2
11	7.16 ddd (8.0, 7.1, 1.1)	122.2
12	7.29 d (8.0)	110.4
13	-	135.3
14	1.68 m	33.5
	1.79 ddd (14.6, 6.5, 1.5)	
15	3.95 br d (4.5)	43.6
16	-	144.7
18	1.68 br d (6.5)	13.5
19	5.65 qt (6.5, 2.0)	120.5
20	-	138.5
21	3.18 d (16.2)	52.5
	3.84 d (16.2)	
22	5.33 d (1.2)	118.0
	5.35 d (1.2)	
CH_2COCH_3	2.10 dd (14.9, 6.5)	51.9
	2.35 dd (14.9, 6.5)	
CH_2COCH_3	1.93 s	30.8
CH_2COCH_3	-	208.6
NH	8.19 br s	-

[a] $CDCl_3$, 400 MHz

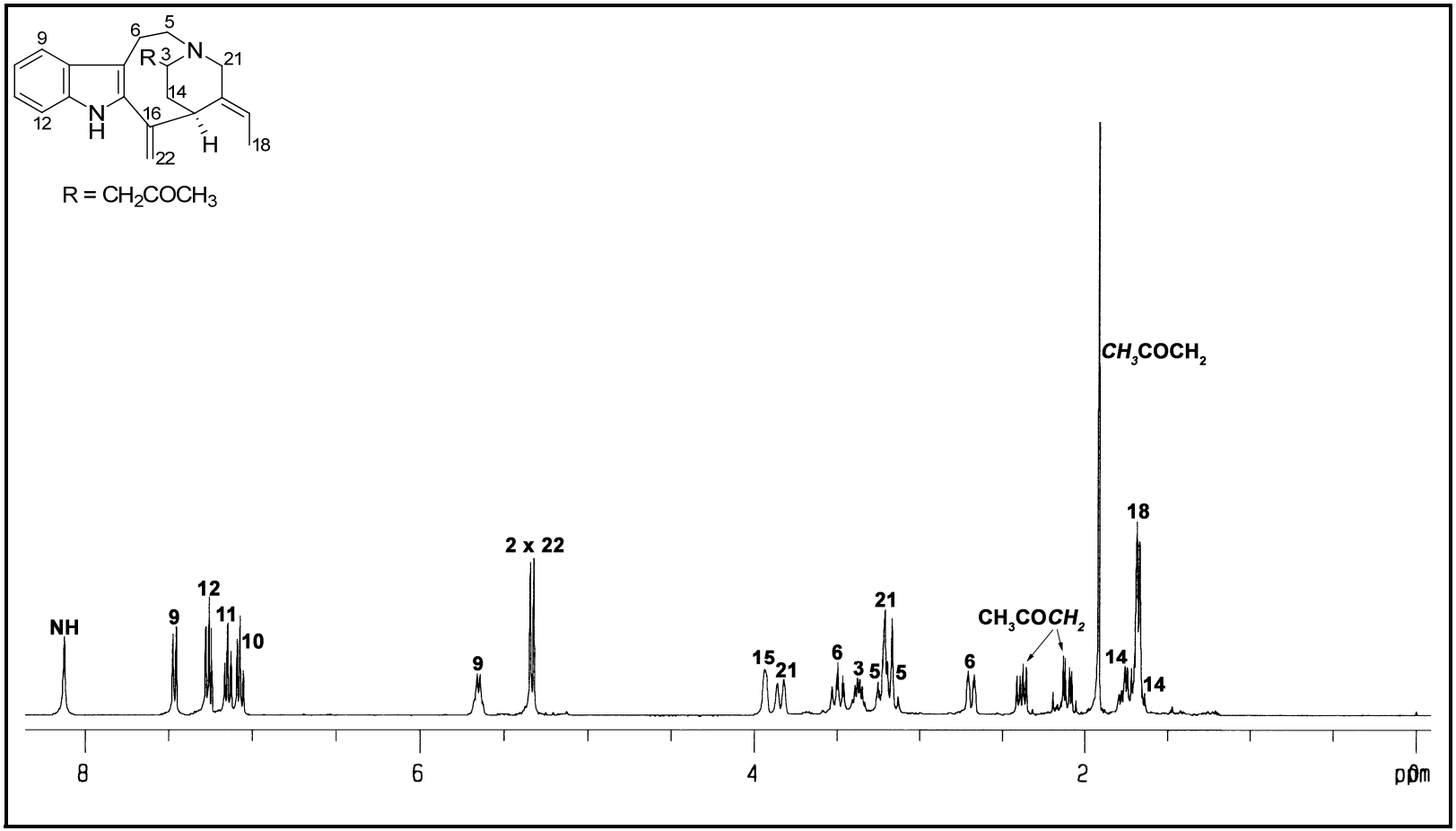

Fig. 2.7: ^{1}H NMR Spectrum ($CDCl_3$, 400 MHz) of 3-Acetonylpericine (**42**)

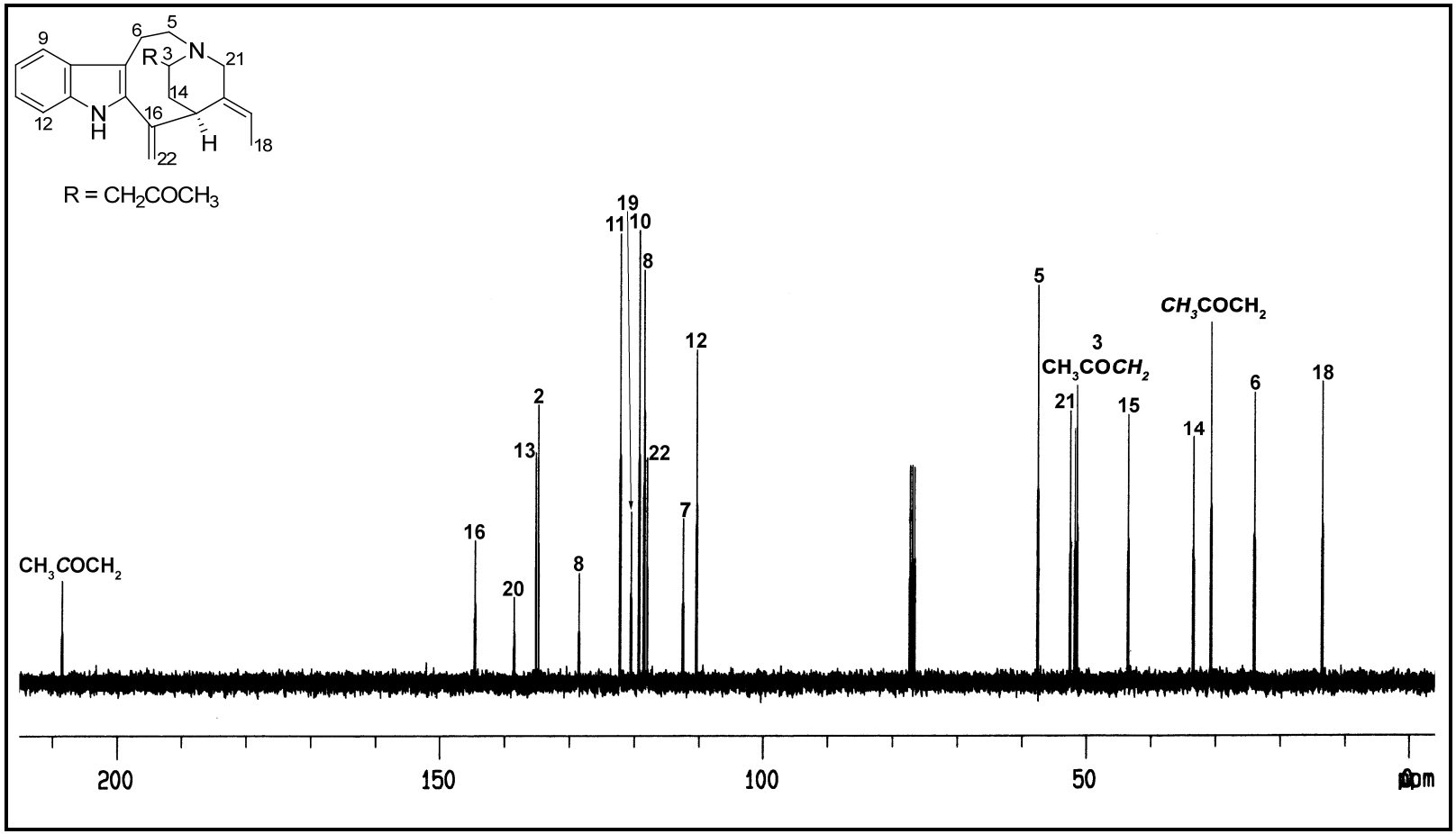

Fig. 2.8: ^{13}C NMR Spectrum ($CDCl_3$, 100 MHz) of 3-Acetonylpericine (**42**)

2.2.2 Application of the Potier-Polonovski Approach to the Biomimetic Transformation of Pericine (31) to Valparicine (28) and Apparicine (29)

In 1927, the Polonovski brothers reported that certain alkaloid N-oxides, upon treatment with acetic anhydride or acetyl chloride, underwent a rearrangement in which one of the alkyl groups attached to the nitrogen was cleaved and the N-acetyl derivative of the alkaloid was obtained.[43] The activation of the tertiary amine N-oxides with acyl halides or anhydride to form the corresponding iminium ion intermediate is known as the Polonovski reaction. When trifluoroacetic anhydride (TFAA) was used as the activation agent, the reaction proceeds under mild conditions (Potier-Polonovski reaction), which then undergoes readily N-O bond cleavage, leading to fragmentation products.[40,44,45]

The first step in the Potier-Polonovski approach to the biomimetic transformation of pericine (**31**) to valparicine (**28**) and apparicine (**29**) involves oxidation of **31** to its N-oxide (**43**), using *m*-chloroperbenzoic acid (*m*-CPBA) in CH_2Cl_2 at 0 ^oC (Scheme 2.4).

Pericine *N*-oxide (**43**) was obtained in 85% yield as colorless crystals (mp 205–208 ^oC), with $[\alpha]_D$ +71 (*c* 0.21, $CHCl_3$). The UV spectrum (227 and 301 nm) showed absorption maxima characteristic of an indole chromophore, while the IR spectrum showed the presence of an NH (3378 cm^{-1}) function. The EIMS of **43** showed an M^+ at *m/z* 294, which analyzed for $C_{19}H_{22}N_2O$ (16 mass units higher than that of **31**). The NMR spectroscopic data showed the characteristic downfield shifts of the carbon resonances for C-3, C-5, and C-21, when compared with those of **31**. The ^1H and ^{13}C NMR spectral data of **43** are summarized in Table 2.4, and the ^1H and ^{13}C NMR spectra of **43** are shown in Fig. 2.9 and Fig. 2.10, respectively.

Table 2.4: ^{1}H and ^{13}C NMR Spectroscopic Data of Pericine *N*-oxide (**43**)[a]

Position	^{1}H	^{13}C
2	-	135.5
3	3.65 dd (14.1, 7)	66.2
	3.90 m	
5	3.72 m	74.9
	3.86 m	
6	3.10 br d (14)	22.6
	3.84 m	
7	-	108.3
8	-	132.3
9	7.42 d (8)	118.1
10	7.13 ddd (8, 7.1, 1.0)	120.2
11	7.22 ddd (8, 7.1, 1.0)	123.2
12	7.37 d (8)	110.8
13	-	135.5
14	1.71 m	26.6
	2.62 tt (14.1, 7)	
15	3.94 m	40.4
16	-	142.0
18	1.75 ddd (7.1, 2.4, 1.7)	13.7
19	5.95 br q (7.1)	127.1
20	-	128.1
21	4.16 d (15)	71.9
	4.43 dt (15, 2.0)	
22	5.43 s	119.0
	5.53 s	
NH	8.62 br s	-

[a]$CDCl_3$, 400 MHz

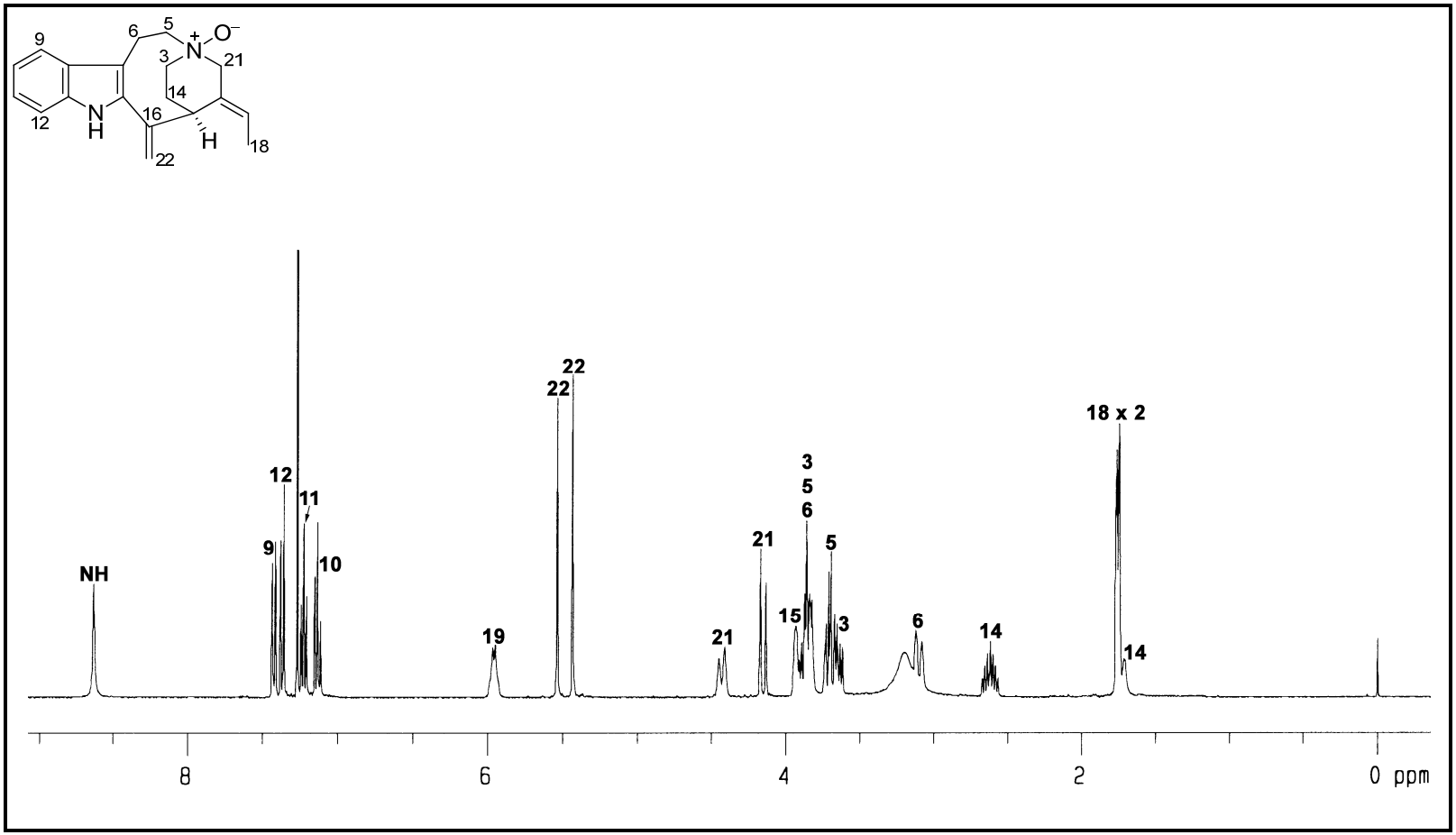

Fig. 2.9: ^{1}H NMR Spectrum ($CDCl_3$, 400 MHz) of Pericine *N*-oxide (**43**)

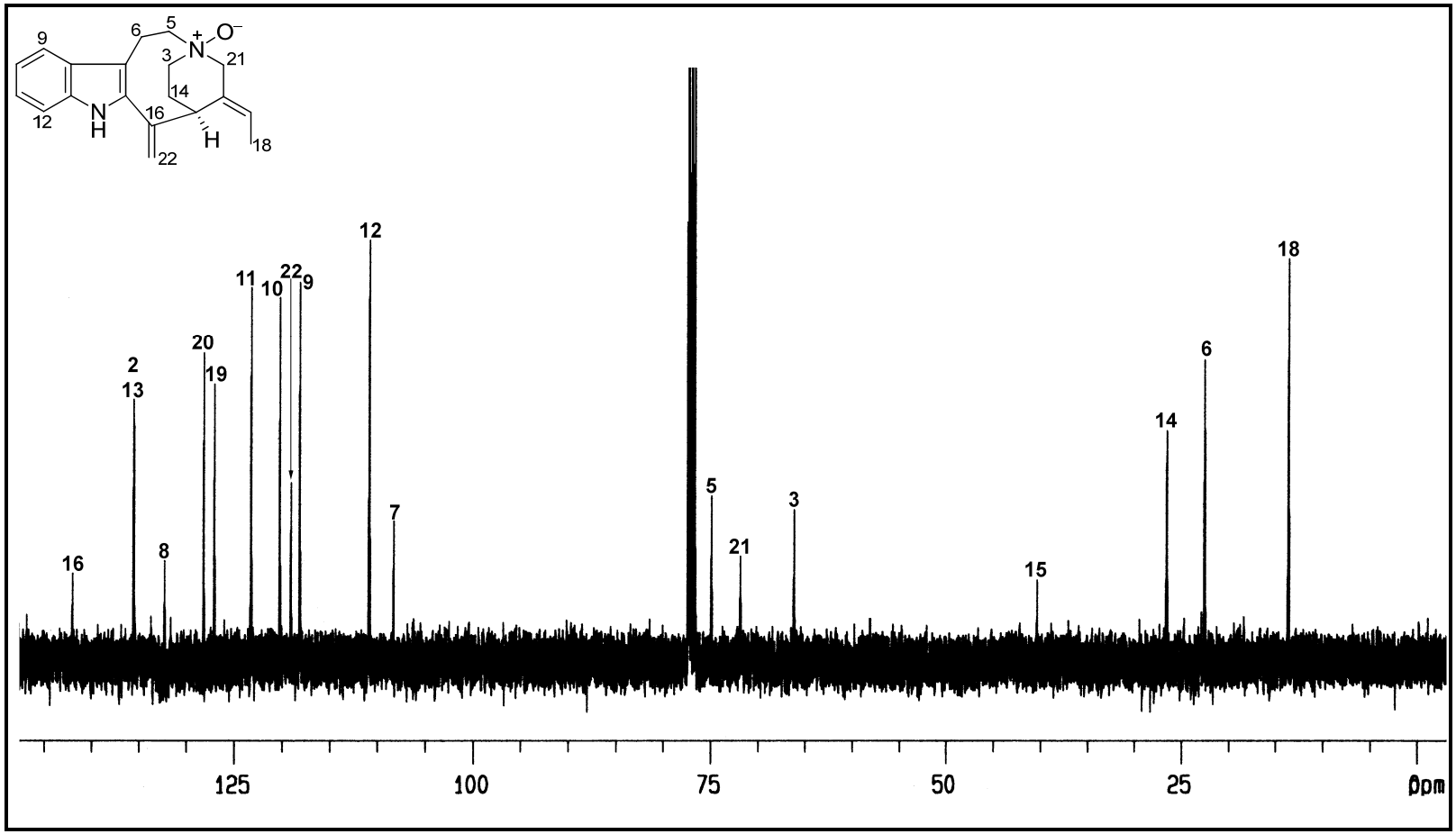

Fig. 2.10: ^{13}C NMR Spectrum ($CDCl_3$, 100 MHz) of Pericine *N*-oxide (**43**)

Pericine *N*-oxide (**43**), on treatment with TFAA in CH_2Cl_2 at −10 ^oC for 30 min, followed by hydrolysis (NaOH) gave two major products in relatively low yields, **28** (4%) and **29** (5%) (Scheme 2.4).

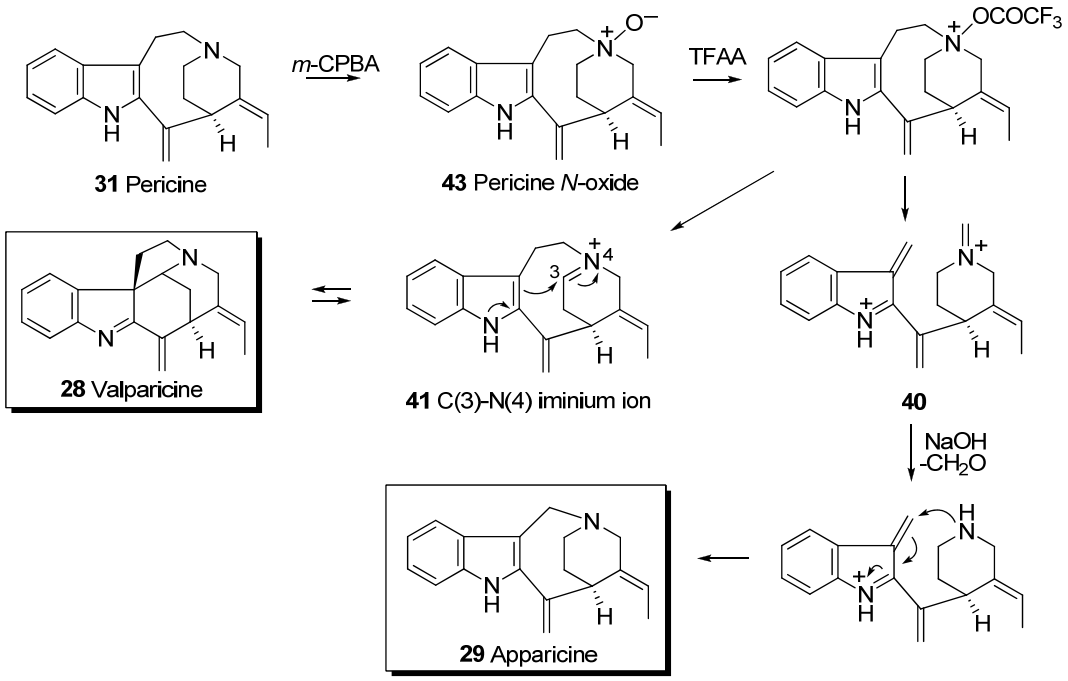

Scheme 2.4

In an attempt to optimize the yields, the various reaction parameters such as concentration, temperature, time of reaction, and amount of TFAA used, were varied (Table 2.5). It can be seen that Entry 15 (Table 2.5) gave the optimum yield.

Table 2.5: Optimization of Reaction Parameters in the Potier-Polonovski Transformation

Entry	Volume of CH_2Cl_2, mL (Concentration, 10^{-2} M)	Temperature (^oC)	Time (minutes)	TFAA (eqv. mol)	Yield (%)		Recovery of **43** (%)
					Valparicine (**28**)	Apparicine (**29**)	
1	4 (4.25)	–10	30	3	5	4	1
2	10 (1.70)	–40	15	8	7	4	2
3	10 (1.70)	0	15	8	9	7	3
4	10 (1.70)	10	15	8	14	7	4
5	10 (1.70)	20	15	8	detected in TLC		-
6	5 (3.40)	10	15	4	2	2	6
7	10 (1.70)	10	5	1.2	7	2	7
8	10 (1.70)	10	10	1.2	7	1	8
9	10 (1.70)	10	20	1.2	9	1	9
10	10 (1.70)	10	10	1.5	6	1	10
11	10 (1.70)	10	10	2	9	3	11
12	50 (0.34)	10	10	1.6	10	1	12
13	50 (0.34)	10	10	2	12	4	13
14	50 (0.34)	10	10	4	16	6	14
15	100 (0.17)	10	10	4	26	10	15
16	100 (0.17)	0	10	4	24	10	16
17	150 (0.13)	10	20	4	17	6	17
18	150 (0.13)	10	10	4	24	9	18

Note: Entry 1–6, TFAA was added into the reaction vessel in one portion; Entry 7–18, TFAA was added into the reaction vessel dropwise; Entry 12, TFAA was diluted with 4 ml of CH_2Cl_2 prior to addition.

In Entries 1–11 (Table 2.5), where the reaction mixtures were relatively concentrated, addition of TFAA into the reaction mixtures resulted in the formation of a dark reddish colored solution. This can be correlated with overreaction, as the overall yields and the recovery of pericine *N*-oxide (**43**) were low in these entries. When TFAA was diluted prior to addition into the reaction chamber (Entry 12, Table 2.5), the overall

yields and the recovery of pericine *N*-oxide (**43**) increased. In addition, unlike Entries 1–11 (Table 2.5) the solution did not turn into the dark reddish color. From these observations, it was deduced that carrying out the reaction at high dilution has a beneficial effect on the overall yield. Thus, from Entry 13 (Table 2.5) onwards, the volume of solvent (CH_2Cl_2) used was increased, and the reaction was optimized at Entry 15 (Table 2.5). Due to paucity of **31**, further optimization was not carried out. Thus, from the experimental data, it can be concluded that high dilution of the reaction mixture is necessary to achieve optimum yields.

In summary, after much experimentation it was found that the overall yield could be raised to about 36% (**28**, 10%; **29**, 26%) by carrying out the reaction at 10 ^{o}C, with 4 equivalent excess of TFAA added dropwise, and at high dilution (100 ml CH_2Cl_2), for 10 min (Entry 15, Table 2.5).

The spectroscopic data (^{1}H and ^{13}C NMR, IR, UV) and other analytical properties ($[\alpha]_D$ and R_f of TLC in different solvent systems) of synthetic **28** and **29** were indistinguishable from those of the natural **28** and **29**.

2.3 Conclusion

The partial synthesis of valparicine (**28**) from the more abundant pericine (**31**) has provided a useful route to the cytotoxic alkaloid which was obtained only in trace amounts from its natural source. This route has provided sufficient quantities of **28** for further evaluation of its cytotoxic effects. In the first of the biological activity studies, valparicine (**28**) was found to show strong cytotoxic effects against both drug-sensitive and vincristine-resistant human KB cells, as well as Jurkat cells (Table 2.6).[27]

The partial synthesis of apparicine (**29**) via the Potier-Polonovski reaction has shown that pericine (**31**) can be considered as a viable intermediate in the biogenetic

pathway to **29**, deriving from stemmadenine (**13**) following deformylation or decarboxylation, and preceding one-carbon extrusion (Scheme 2.1). Such an alternative would be consistent with both the Kutney (one carbon extrusion preceding decarboxylation unlikely)[39] and Scott (one-carbon extrusion and deformylation/decarboxylation steps not necessarily synchronous)[41] results. In addition it has also been shown that **28** is in all probability biogenetically related to **31**. These relationships are summarized in Scheme 2.5. It is, however, somewhat puzzling that **29** was not detected among the many alkaloids obtained from *K. arborea*, although both **28** and **29** have been previously found in *A. subincanum*.[29]

Table 2.6: Cytotoxic Effects of Valparicine (**28**)

	$IC_{50,}$ μg/mL (μM)			
	KB/S (sensitive)	KB/VJ300 (resistant)	KB/VJ300 (0.1μg/ml VCR added)	Jurkat
Valparicine (**28**)	1.1	0.93	0.84	0.21

KB/S = Vincristine-sensitive human oral epidermoid carcinoma cell line.

KB/VJ300 = Vincristine-resistant human oral epidermoid carcinoma cell line.

Jurkat = Human T-cell leukemia cell line.

VCR = Vincristine

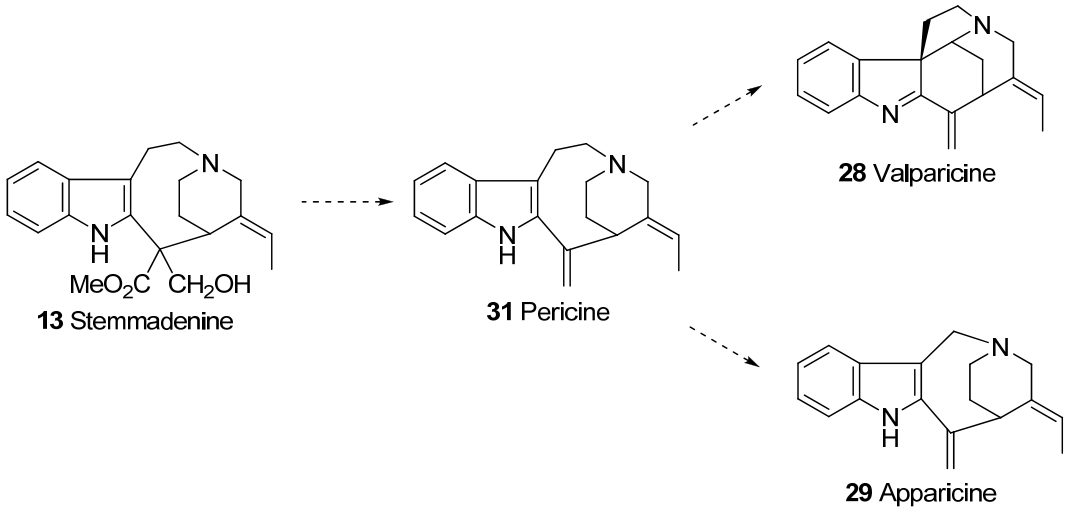

Scheme 2.5